

Fermi National Accelerator Laboratory

FERMILAB-Pub-93/194-E

E687

Study of $D^0 \rightarrow K^- \mu^+ \nu$ in High Energy Photoproduction

P.L. Frabetti et al
the E687 Collaboration

*Fermi National Accelerator Laboratory
P.O. Box 500, Batavia, Illinois 60510*

July 1993

Submitted to *Physics Letters B*

Disclaimer

This report was prepared as an account of work sponsored by an agency of the United States Government. Neither the United States Government nor any agency thereof, nor any of their employees, makes any warranty, express or implied, or assumes any legal liability or responsibility for the accuracy, completeness, or usefulness of any information, apparatus, product, or process disclosed, or represents that its use would not infringe privately owned rights. Reference herein to any specific commercial product, process, or service by trade name, trademark, manufacturer, or otherwise, does not necessarily constitute or imply its endorsement, recommendation, or favoring by the United States Government or any agency thereof. The views and opinions of authors expressed herein do not necessarily state or reflect those of the United States Government or any agency thereof.

Study of $D^0 \rightarrow K^- \mu^+ \nu$ in High Energy Photoproduction

P.L. Frabetti

Dip. di Fisica dell'Università and INFN - Bologna, I-40126 Bologna, Italy

C. W. Bogart^(a), H. W. K. Cheung, S. Culy, J. P. Cumalat, W. E. Johns
University of Colorado, Boulder, CO 80309, USA

J. N. Butler, F. Davenport^(b), I. Gaines, P. H. Garbincius, S. Gourlay, D. J. Harding,
P. Kasper, A. Kreymer, P. Lebrun, H. Mendez^(c)
Fermilab, Batavia, IL 60510, USA

S. Bianco, M. Enorini, F. L. Fabbri, A. Spallone, A. Zallo
Laboratori Nazionali di Frascati dell'INFN, I-00044 Frascati, Italy

R. Culbertson, G. Jaross^(d), K. Lingel^(e), P. D. Sheldon^(f), J. R. Wilson^(g), J. Wiss
University of Illinois at Urbana-Champaign, Urbana, IL 61801, USA

G. Alimonti, D. Alliata, G. Bellini, M. Di Corato, M. Giammarchi, D. Hazan, P. Inzani, F. Leveraro,
S. Malvezzi, D. Menasce, E. Meroni, L. Moroni, D. Pedrini, L. Perasso, A. Sala,
S. Sala, D. Torretta^(h), M. Vittone^(h)
Dip. di Fisica dell'Università and INFN - Milano, I-20133 Milan, Italy

D. Buchholz, C. Castoldi⁽ⁱ⁾, B. Gobbi, S. Park^(h), R. Yoshida^(j)
Northwestern University, Evanston, IL 60208, USA

J.M. Bishop, J.K. Busenitz^(k), N.M. Cason, J.D. Cunningham^(l), R.W. Gardner^(m), C.J. Kennedy⁽ⁿ⁾,
E. J. Mannel^(o), R. J. Mountain^(p), D. L. Puseljc, R. C. Ruchti, W. D. Shephard, M. E. Zanabria
University of Notre Dame, Notre Dame, IN 46556, USA

S. P. Ratti, P. Vitulo

Dip. di Fisica Nucleare e Teorica and INFN - Pavia, I-27100 Pavia, Italy

A. Lopez

University of Puerto Rico at Mayaguez, Puerto Rico

(E687 Collaboration)

Present addresses: ^(a) Acoustic Signal Processing, Code 7123, Naval Research Laboratory 4555 Overlook Ave SW Washington DC 20375, USA; ^(b) University of North Carolina-Asheville, Asheville, NC 28804, USA; ^(c) University of Illinois at Chicago, Chicago, IL 60680, USA; ^(d) STX Inc., 4400 Forbes Blvd., Lanham, MD 20706, USA; ^(e) University of Colorado, Boulder, CO 80309, USA; ^(f) Vanderbilt University, Nashville, TN 37235, USA; ^(g) University of South Carolina, Columbia, SC 29208, USA; ^(h) Fermilab, Batavia, IL 60510, USA; ⁽ⁱ⁾ INFN - Pavia, I-27100 Pavia, Italy; ^(j) NIKHEF-H, 1009 DB, Amsterdam, The Netherlands; ^(k) University of Alabama, Tuscaloosa, AL 35487, USA; ^(l) Brandeis University, Waltham, MA 02254, USA; ^(m) University of Illinois at Urbana-Champaign, Urbana, IL 61801, USA; ⁽ⁿ⁾ Yale University, New Haven, CN 06510, USA; ^(o) Nevis Labs, Columbia University, Irvington, NY 10533, USA; ^(p) Syracuse University, Syracuse, NY 13244-1130, USA.

Abstract

We report a measurement of the semimuonic decay $D^0 \rightarrow K^- \mu^+ \nu$ from data taken during the 1987-1988 fixed target run at Fermilab by the E687 collaboration. We obtain $\Gamma(D^0 \rightarrow K^- \mu^+ \nu) / \Gamma(D^0 \rightarrow K^- \pi^+) = 0.82 \pm 0.13 \pm 0.13$ and use this result to calculate $\Gamma(D^0 \rightarrow K^{*-} \mu^+ \nu) / \Gamma(D^0 \rightarrow K^- \mu^+ \nu) = 0.59 \pm 0.10 \pm 0.13$.

The semileptonic decays of charmed particles are particularly interesting as they proceed via the spectator model and the matrix element can be factorized into a hadronic part and a well understood leptonic part. As a result the decay rate for the pseudoscalar and the vector semileptonic decays is straightforward to calculate. However, both the decay rate $\Gamma(D \rightarrow K^* \mu^+ \nu)$ and the branching fraction $\Gamma(D \rightarrow K^* \mu^+ \nu)/\Gamma(D \rightarrow K \mu^+ \nu)$ disagree with many theoretical predictions^{[1],[2]}. In this study a measurement is made of $\Gamma(D^0 \rightarrow K^- \mu^+ \nu)/\Gamma(D^0 \rightarrow K^- \pi^+)$ † and, utilizing our previous^[3] measurement of the ratio $\Gamma(D^+ \rightarrow K^{*0} \mu^+ \nu)/\Gamma(D^+ \rightarrow K^- \pi^+ \pi^-)$, a calculation is made of $\Gamma(D^0 \rightarrow K^{*-} \mu^+ \nu)/\Gamma(D^0 \rightarrow K^- \mu^+ \nu)$.

The E687 detector^[4] is a large aperture, multiparticle magnetic spectrometer with excellent vertex measurement, momentum resolution, and particle identification. The average triggered photon energy is 221 GeV. For this analysis 60 million multihadronic triggers from the 1987-1988 run have been analyzed.

The $D^0 \rightarrow K^- \mu^+ \nu$ candidates were skimmed from the reconstructed data tapes by requiring evidence for multiple vertices. An event is included in the skim sample if it contains at least two vertices separated by at least 3 standard deviations. As the neutrino is not directly detected, the positions of the primary and secondary vertices are used to calculate the neutrino's transverse momentum and the assumed D^0 mass is exploited to determine the longitudinal momentum.

Two track secondary vertices are chosen from oppositely charged tracks where one track is identified as a muon and the other is identified as a kaon. In order to eliminate pion and kaon decay backgrounds as well as particle misidentification, a minimum muon momentum of 10 GeV/c is required.

† In this report reference to particles like D^{*+} , D^+ and D^0 , implies also the charge conjugate state.

The primary vertex is constructed after removing the tracks belonging to the $K\mu$ vertex (secondary vertex). The primary vertex is required to be upstream of the secondary vertex and in the target region. The primary vertex must also include at least three tracks and contain one track consistent with being a pion in the Čerenkov system. If more than one primary vertex candidate satisfies the above cuts, the highest multiplicity vertex is chosen. If two or more vertices have the same number of tracks, then the most upstream primary vertex within the target region is selected.

A secondary vertex detachment cut of $\ell/\sigma_\ell \geq 5$ is introduced to reject the non-charm backgrounds (ℓ is the distance between the primary and the secondary vertex; σ_ℓ is its error ^[4]). Higher multiplicity decay channels are eliminated from this sample by requiring other tracks not associated with the primary vertex to have less than a 2% confidence level of belonging to the $K\mu$ vertex.

As we cannot directly detect the neutrino, we exploit the $D^{*+} \rightarrow D^0 \pi^+$ decay followed by $D^0 \rightarrow K^- \mu^+ \nu$. The line between the primary and secondary vertex determines the D^0 flight direction. Using this flight direction and assuming $M_{K\mu\nu} = M_{D^0}$ and $M_\nu = 0$, the longitudinal component of the neutrino momentum is calculated in the reference frame where the $K\mu$ longitudinal momentum along the D^0 direction is zero^[5]. When vertex resolution is included it is possible to have unphysical values for the D^0 momentum, hence slightly negative values are allowed ($(\vec{P}_\nu \cdot \vec{l})^2 = (E_\nu^2 - P_{K\mu}^2) > -0.7 \text{ (GeV/c)}^2$). For those cases with $-0.7 < (E_\nu^2 - P_{K\mu}^2) < 0$ it is set $(E_\nu^2 - P_{K\mu}^2) = 0$ (\vec{l} is the direction of the D^0 in the boosted frame). Whenever two solutions are kinematically possible, the case with the lowest D^{*+} mass is selected. The π^+ candidates are required to belong to the primary vertex and to have a momentum less than 13.5 GeV/c.

Figure 1 displays the $K^-\mu^+\nu\pi^+$ invariant mass distribution (solid line) obtained with $M_{K\mu\nu} = M_{D^0}$ and with a $\ell/\sigma_\ell \geq 5$ requirement. The random background (dotted line) is obtained from events where the soft pion has opposite charge from the muon.

Several background contamination sources were considered. The largest background was found to be $D^0 \rightarrow K^{*-}\mu^+\nu$ where the $K^{*-} \rightarrow K^-\pi^0$ with the π^0 not reconstructed. Other backgrounds considered were $D^0 \rightarrow (K^-\pi^+)\pi^0$ (resonant and non-resonant) and $D^0 \rightarrow K^-\pi^+\pi^0\pi^0$ where the π^+ decays to $\mu^+\nu$ or is misidentified as a μ^+ (with a probability of 1.7 %).

To separate the contribution in the D^* peak due to the semileptonic decay from that due to other charm decay channels, a Monte Carlo $K\mu\nu\pi$ invariant mass distribution was created (MC_{tot}) that summed the decay of interest, the other charm channels listed in table I, and the normalized combinations taken from the wrong sign events in the data.

The branching fraction of $D^0 \rightarrow K^-\mu^+\nu$ relative to the channel $D^0 \rightarrow K^-\pi^+$, both observed via the decay chain $D^{*+} \rightarrow \pi^+D^0$, can be written as:

$$\frac{\Gamma(D^0 \rightarrow K^-\mu^+\nu)}{\Gamma(D^0 \rightarrow K^-\pi^+)} = \frac{BR(D^0 \rightarrow K^-\mu^+\nu)}{\sum_i(BR_i)} \cdot \frac{N_{D^{*+}peak}^{obs}}{\sum_i(BR_i \cdot \epsilon_i) / \sum_i(BR_i)} \cdot \frac{\epsilon_{K\pi}}{N_{K\pi}^{obs}}$$

where $\epsilon_{K\pi}$ is the Monte Carlo reconstruction efficiency, $N_{K\pi}^{obs}$ is the number of observed events for the $D^0 \rightarrow K^-\pi^+$ decay, and $\sum_i(BR_i \cdot \epsilon_i) = (BR_{K\mu\nu} \cdot \epsilon_{K\mu\nu} + BR_{K^*\mu\nu} \cdot \epsilon_{K^*\mu\nu} + BR_{K\pi\pi^0} \cdot \epsilon_{K\pi\pi^0} + BR_{K\pi\pi^0\pi^0} \cdot \epsilon_{K\pi\pi^0\pi^0})$ with Monte Carlo calculated efficiencies and known branching ratios^[6] (all but the unknown $BR_{K\mu\nu}$) given in table I. The term $\sum_i(BR_i \cdot \epsilon_i) / \sum_i(BR_i)$ is the effective detection and reconstruction efficiency for the composite D^{*+} state. The term $BR(D^0 \rightarrow K^-\mu^+\nu) / \sum_i(BR_i)$ is the fraction of the D^{*+} peak consisting of the $K^-\mu^+\nu$ state.

In order to properly account for the effects of resolutions and backgrounds on the observed D^{*+} peak, an iterative approach is used to obtain the $BR_{K\mu\nu}$ value.

In the first iteration, the $BR_{K\mu\nu}$ value is fixed and the D^{*+} peak is fit with MC_{tot} , which is now a function of $BR_{K\mu\nu}$. Next, using the measured $N_{D^{*+}peak}^{obs}$ a new value of $BR_{K\mu\nu}$ is calculated. This new result is then used to create another Monte Carlo distribution and the procedure is iterated until the $BR_{K\mu\nu}$ input value is equal to the $BR_{K\mu\nu}$ output value. The result of the fit, shown in figure 1, yields 99 ± 14 signal events (after background subtraction) for the total number of $K^-\mu^+\nu$ decays in the D^* peak.

The $D^{*+} \rightarrow D^0\pi^+ \rightarrow (K^-\pi^+)\pi^+$ channel is used as the normalization channel. This channel is selected from the same data skim, uses the same vertexing algorithms, and has the same analysis cuts applied where possible. Figure 2a) shows the $((K^-\pi^+)\pi^+)$ invariant mass distribution when $1.834 < M_{K^-\pi^+} < 1.894 \text{ GeV}/c^2$ and where $M_{K\pi} = M_{D^0}$. Figure 2b) presents the $K^-\pi^+$ invariant mass distribution. A signal yield of 210 ± 17 events is obtained after subtracting the wrong sign contribution $((K^-\pi^+)\pi^-)$. The efficiency for this decay is measured to be $\epsilon_{K\pi} = 3.63\%$.

The background contamination signal from $D^0 \rightarrow K^-K^+$, where a K decays to $\mu\nu$ or is misidentified as a π , has been determined to be negligible compared with the other backgrounds.

Hence, the relative branching ratio is found to be:

$$\frac{\Gamma(D^0 \rightarrow K^-\mu^+\nu)}{\Gamma(D^0 \rightarrow K^-\pi^+)} = 0.82 \pm 0.13(stat.) \pm 0.13(syst.)$$

As a check that the contamination from decays with missing π^0 's and misidentified muons is understood, the $K\mu$ invariant mass distribution for the data is compared with the Monte Carlo predictions. The total contamination in the sample from the charm background channels is found to be 25 ± 5 events, of which 11 events are estimated to be from the $D^0 \rightarrow K^{*-}\mu^+\nu$ decay and 14 events from the $D^0 \rightarrow (K^-\pi^+)\pi^0$ and $D^0 \rightarrow K^-\pi^+\pi^0\pi^0$ decays. Figure 3 displays the $M(K\mu)$ mass dis-

tribution after the wrong sign background has been subtracted for $2.005 < M_{K\mu\nu\pi} < 2.025 \text{ GeV}/c^2$. As expected the background peaks at a lower $M_{K\mu}$ mass than the signal. The Monte Carlo simulation is in good agreement with the data.

The systematic errors were estimated by varying the choice of the kinematic, detachment and isolation cuts, by considering the branching fraction uncertainties in the PDG values, by changing the normalization procedures, and by studying the effect of an $M_{K\mu}$ cut to aid in reducing π decays and to help eliminate the charm decays with more than one neutral. The errors were added in quadrature.

Figure 4 shows the D^* yield as a function of the secondary vertex confidence level cut. The Monte Carlo prediction is superimposed. At low confidence level there is contamination from events where the K and μ do not originate from the same decay. A secondary vertex confidence level cut of 5% is used.

From figure 5 it is observed that the choice of the detachment cut (l/σ_l) is not critical in measuring this branching ratio.

Using the Particle Data Group $BF(D^0 \rightarrow K^- \pi^+) = 3.65 \pm 0.21\%$ ^[6] value, a branching fraction for $D^0 \rightarrow K^- \mu^+ \nu$ of $2.99 \pm 0.47 \pm 0.50\%$ is calculated. Figure 6 compares the E687 result to the branching fractions obtained by other experiments in both the $(K e \nu)$ and in the $(K \mu \nu)$ channels; the electron results are all higher than the muon results as expected from the difference in the lepton masses.

The branching ratio $\Gamma(D^0 \rightarrow K^{*-} \mu^+ \nu)/\Gamma(D^0 \rightarrow K^- \mu^+ \nu)$ is evaluated using the value $\Gamma(D^+ \rightarrow \bar{K}^{*0} \mu^+ \nu)/\Gamma(D^+ \rightarrow K^- \pi^+ \pi^+) = 0.56 \pm 0.04 \pm 0.06$ obtained in this same experiment^[3] from the 1990 run data sample. The calculation is made using the world average values for the D^0 and D^+ lifetimes^[6], the hypothesis $\Gamma(D^0 \rightarrow K^{*-} \mu^+ \nu) = \Gamma(D^+ \rightarrow \bar{K}^{*0} \mu^+ \nu)$, and the PDG values for $\Gamma(D^0 \rightarrow K^- \pi^+)$ and $\Gamma(D^+ \rightarrow K^- \pi^+ \pi^+)$.

The result is found to be:

$$\frac{\Gamma(D^0 \rightarrow K^{*-}\mu^+\nu)}{\Gamma(D^0 \rightarrow K^-\mu^+\nu)} = 0.59 \pm 0.10 \pm 0.13.$$

If the Mark III branching fractions^[10] of $BR(D^0 \rightarrow K^-\pi^+) = 4.2 \pm 0.4 \pm 0.4\%$ and $BR(D^+ \rightarrow K^-\pi^+\pi^+) = 9.1 \pm 1.3 \pm 0.4\%$ are used, then a similar value of $0.58 \pm 0.10 \pm 0.16$ is found.

Figure 7 shows this result with those from other experiments. This result agrees with the other results.

Acknowledgement

We wish to acknowledge the assistance of the staff of Fermi National Accelerator Laboratory, the I.N.F.N. of Italy, and the staffs of the physics departments of the collaborating institutions. This research was supported in part by the National Science Foundation, the U.S. Department of Energy, the Italian Istituto Nazionale di Fisica Nucleare and Ministero dell'Università e della Ricerca Scientifica e Tecnologica.

References

- [1] see references in S.Stone contribution in "Heavy Flavours", ed. by A. J. Buras and H. Lindner, World Scientific, Singapore (1992).
- [2] D. Potter, Proceedings of the 1991 International Lepton-Photon Symposium and Europhysics Conference on High Energy Physics, (World Scientific, 1992) 528.
- [3] E687 Collab., P. L. Frabetti et. al., Phys. Lett. B307 (1993) 262.
- [4] E687 Collab., P. L. Frabetti et al., Nucl. Instrum. Methods A320 (1992) 519.
- [5] E691 Collab., J. C. Anjos et al., Phys. Rev. Lett. 62 (1989) 1587.
- [6] Particle Data Group, K. Hikasa et al., Phys. Rev. D45 S1 (1992).
- [7] CLEO Collab., G. Crawford et al., Phys. Rev. D44 (1991) 3394.

- [8] Mark III Collab., J. Adler et al., Phys. Rev. Lett. 62 (1989) 1821.
- [9] E653 Collab., K. Kodama et al., Phys. Rev. Lett. 66 (1991) 1819.
- [10] Mark III Collab., J. Adler et al., Phys. Rev. Lett. 66 (1988) 89.
- [11] Mark III Collab., Z. Bai et al., Phys. Rev. Lett. 66 (1991) 1011.
- [12] E691 Collab., J. C. Anjos et al., Phys. Rev. Lett. 67 (1991) 1507.
- [13] E653 Collab., K. Kodama et al., Phys.Lett. B286 (1992) 187.
- [14] Mark III Collab.: J. Izen, private communication.

Figure Captions

Table I: contributions from other charm decays.

Fig. 1: $K\mu\nu\pi$ invariant mass distribution for the events satisfying the $\ell/\sigma_\ell > 5$ condition, secondary vertex isolation cut ≤ 0.02 and secondary vertex confidence level $\geq 5\%$, where the $M(K\mu\nu)$ has been set equal to the D^0 mass. The histograms are: the r.s. data (full line) and the w.s. data (dashed line) normalized to the r.s. for $M_{K\mu\nu\pi} \geq 2.025$ GeV/c². Superimposed are the signal fit result (full line) and the random background fit (dotted line).

Fig. 2: a) The $K^-\pi^+\pi^+$ invariant mass where the $M_{K^-\pi^+}$ has been set equal to the D^0 mass; the shaded area is the wrong sign events; b) $K^-\pi^+$ invariant mass for the normalization channel.

Fig. 3: $K\mu$ invariant mass distributions: the open circles are the data values for the events in the D^* peak (wrong sign subtracted); the lines are the Monte Carlo predictions for the signal $D^0 \rightarrow K\mu\nu$ (dashed line), for the sum of backgrounds $D^0 \rightarrow K^{*-}\mu^+\nu$, $D^0 \rightarrow (K^-\pi^+)\pi^0$ and $D^0 \rightarrow K^-\pi^+\pi^0\pi^0$ decays (dotted line), and the sum of all the considered decays, signal plus backgrounds (full line).

Fig. 4: Number of events in the D^* peak (random background subtracted) as a function of the secondary vertex confidence level; the full line is the Monte Carlo prediction; the cut chosen is 0.05.

Fig. 5: Branching ratio value as a function of the ℓ/σ_ℓ cut.

Fig. 6: Comparison of $BF(D^0 \rightarrow K^-\ell^+\nu)$ measurements (values are in %): the statistical (full line) and systematic errors are summed linearly (dashed line). The E691^[5] and CLEO^[7] values have been obtained using the Mark III value for the $BF(D^0 \rightarrow K^-\pi^+)$; E653^[9] calculates this value from the branching ratio $\Gamma(D^0 \rightarrow K\mu\nu)/\Gamma(D^0 \rightarrow X\mu\nu)$.

Fig. 7: Comparison of $\Gamma(D^0 \rightarrow K^{*-}l^+\nu)/\Gamma(D^0 \rightarrow K^-l^+\nu)$ measurements: the statistical (full line) and systematic errors are summed linearly (dashed line). Mark III value refers to the $Kl4/Kl3$ ratio: they do not have sufficient sensitivity to quote a branching fraction ratio for the $D^0 \rightarrow K^{*-}l^+\nu$ ^[14].

Table I: Contributions from Charm Decays:

Background Decay	Branching fraction (%) from PDG ^[6]	$\epsilon(\%)$
$D^0 \rightarrow K^* \mu \nu$	1.7 ± 0.6	0.38
$D^0 \rightarrow K \pi \pi^0$ (res. and non res.)	11.3 ± 1.1	0.03
$D^0 \rightarrow K \pi \pi^0 \pi^0$	15 ± 5	0.03
Signal Decay	Branching fraction (%)	
$D^0 \rightarrow K \mu \nu$	$2.99 \pm 0.5 \pm 0.5$ (this result)	1.56
	2.90 ± 0.5 (from PDG ^[6])	

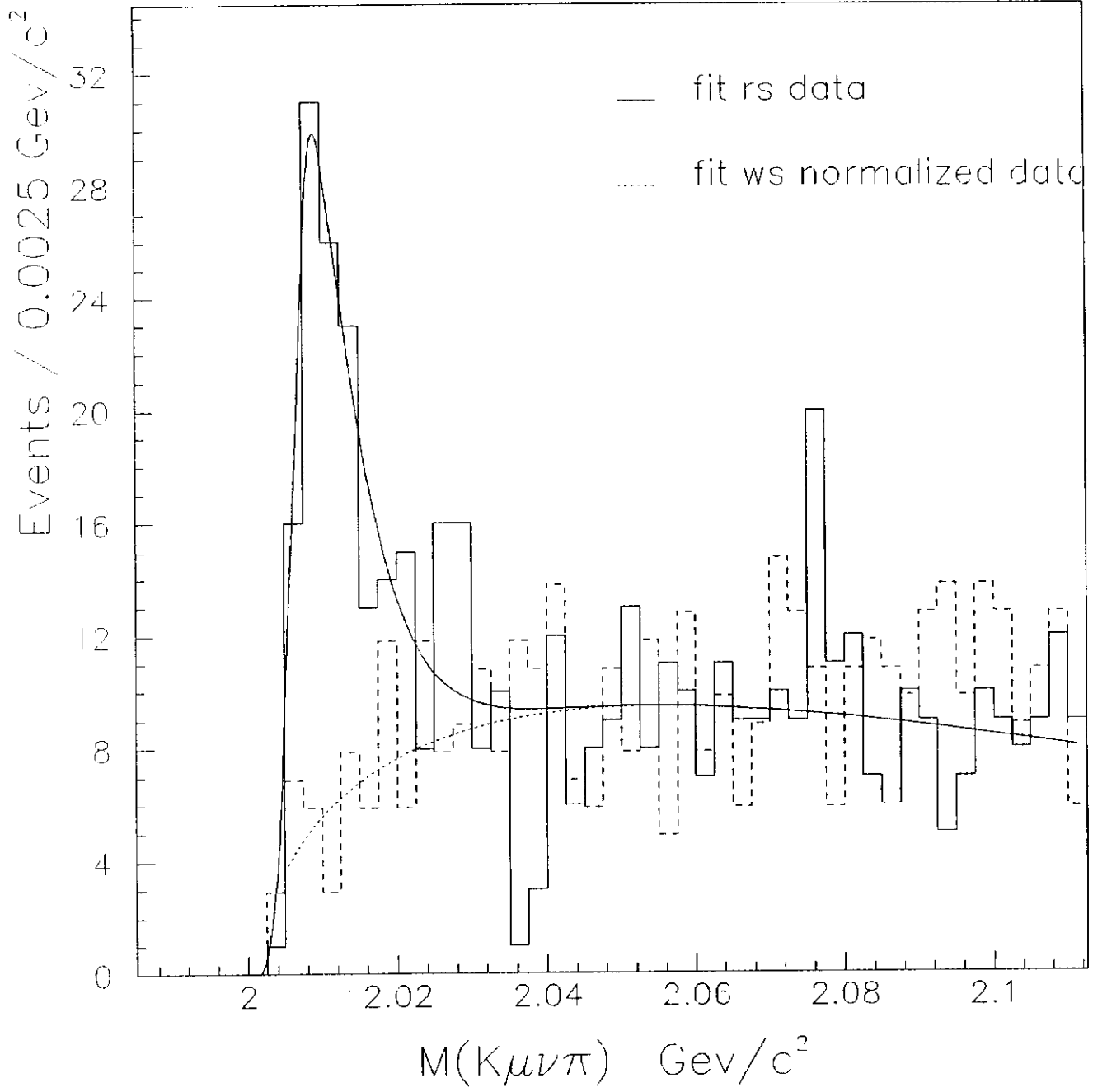


Fig. 1: $K\mu\nu\pi$ invariant mass distribution for the events satisfying the $\ell/\sigma_\ell > 5$ condition, secondary vertex isolation cut ≤ 0.02 and secondary vertex confidence level $\geq 5\%$, where the $M(K\mu\nu)$ has been set equal to the D^0 mass. The histograms are: the r.s. data (full line) and the w.s. data (dashed line) normalized to the r.s. for $M_{K\mu\nu\pi} \geq 2.025 \text{ GeV}/c^2$. Superimposed are the signal fit result (full line) and the random background fit (dotted line).

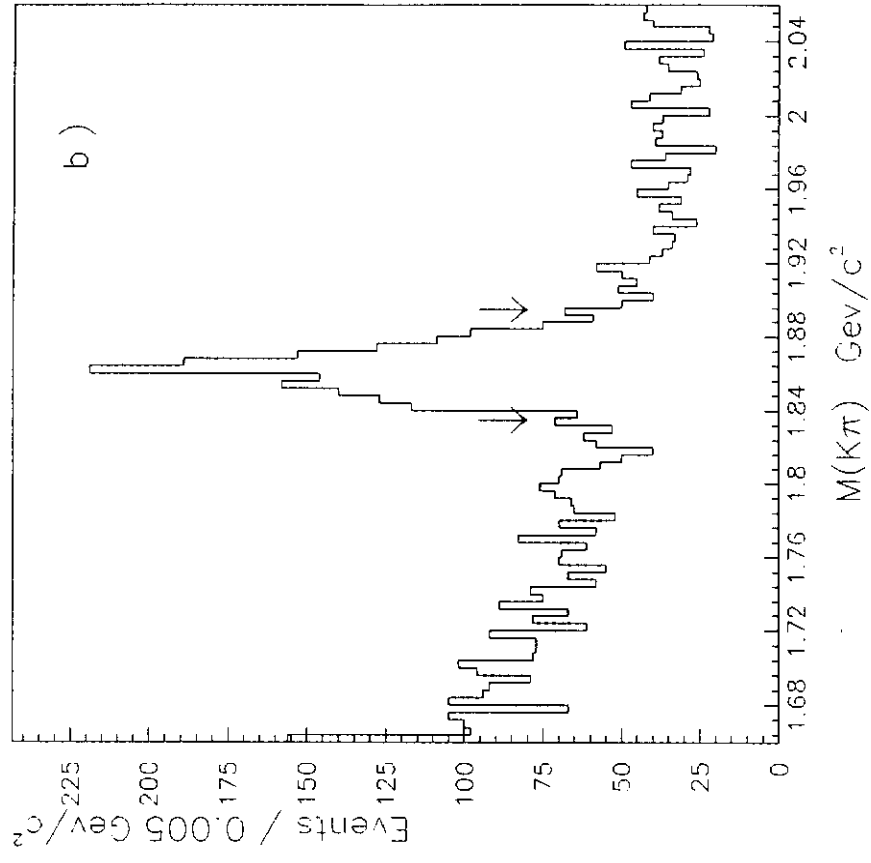
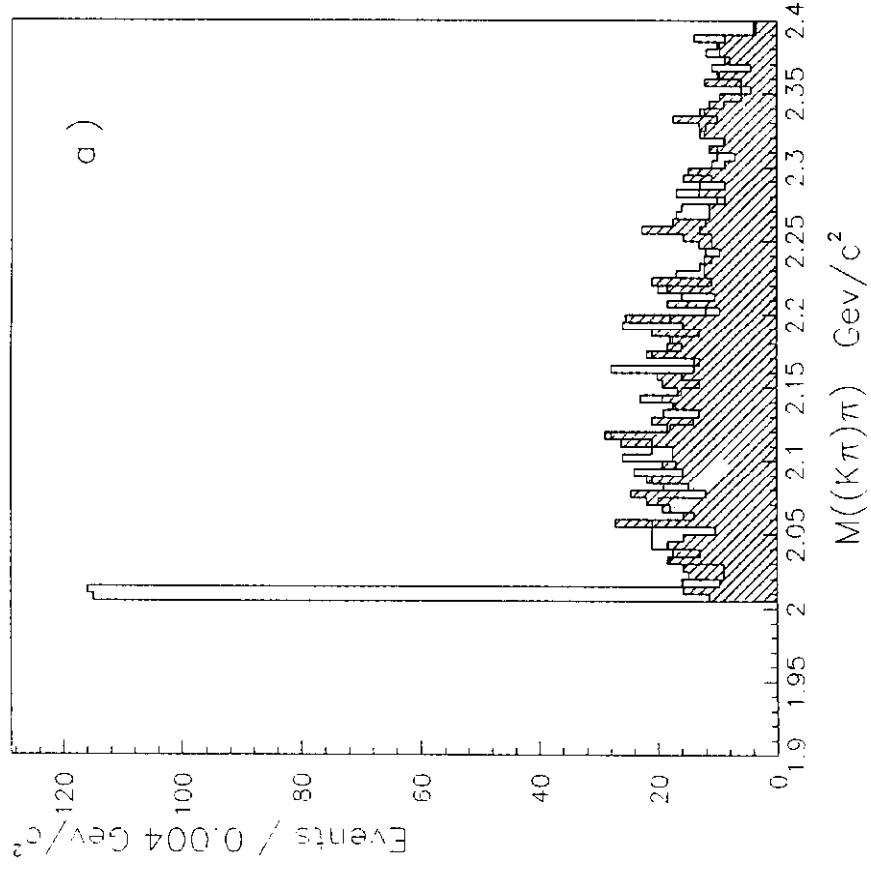


Fig. 2: a) The $K^- \pi^+ \pi^+$ invariant mass where the $M_{K^- \pi^+}$ has been set equal to the D^0 mass; the shaded area is the wrong sign events; b) $K^- \pi^+$ invariant mass for the normalization channel.

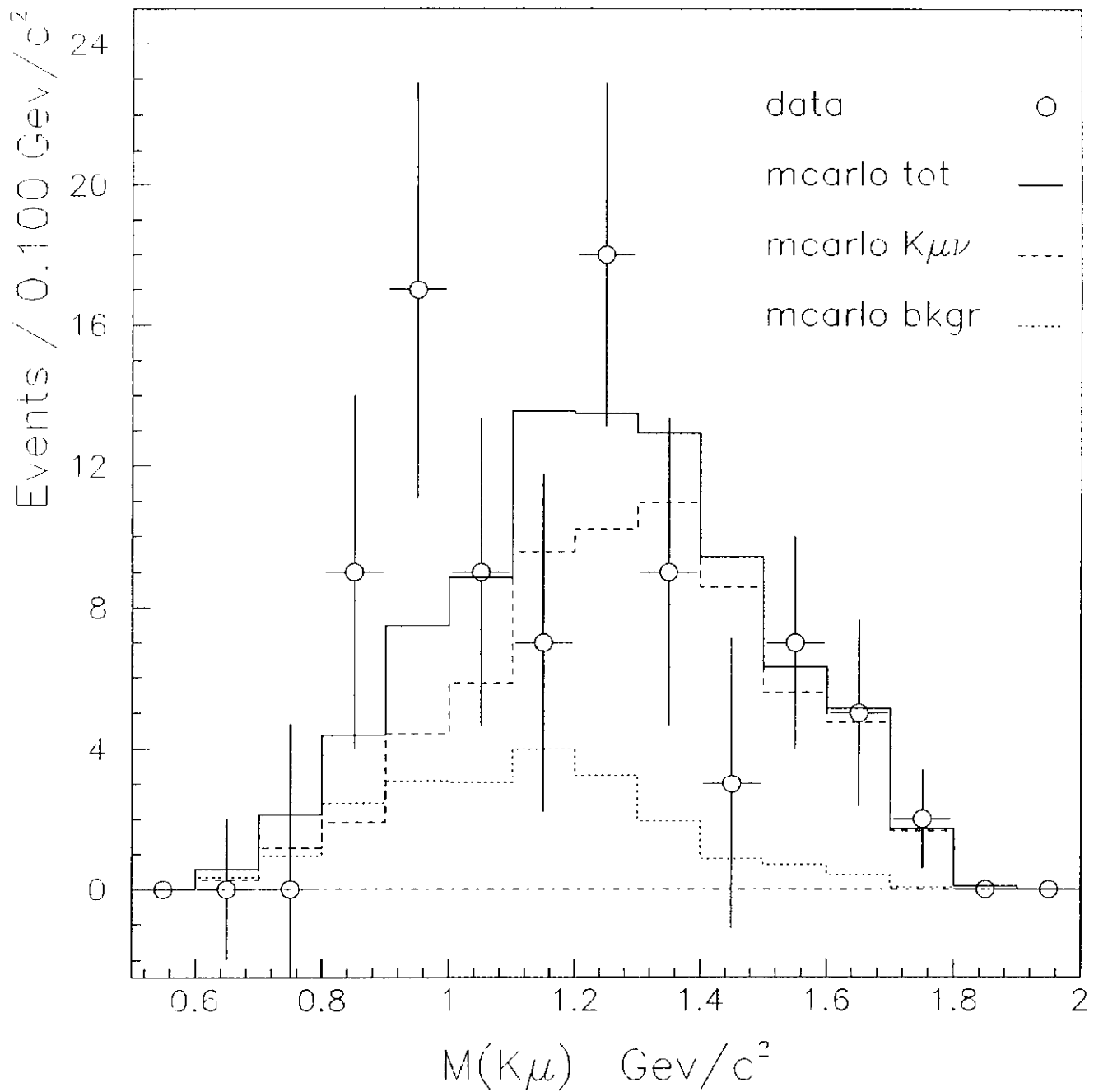


Fig. 3: $K\mu$ invariant mass distributions: the open circles are the data values for the events in the D^* peak (wrong sign subtracted); the lines are the Monte Carlo predictions for the signal $D^0 \rightarrow K\mu\nu$ (dashed line), for the sum of backgrounds $D^0 \rightarrow K^{*-}\mu^+\nu$, $D^0 \rightarrow (K^-\pi^+)\pi^0$ and $D^0 \rightarrow K^-\pi^+\pi^0\pi^0$ decays (dotted line), and the sum of all the considered decays, signal plus backgrounds (full line).

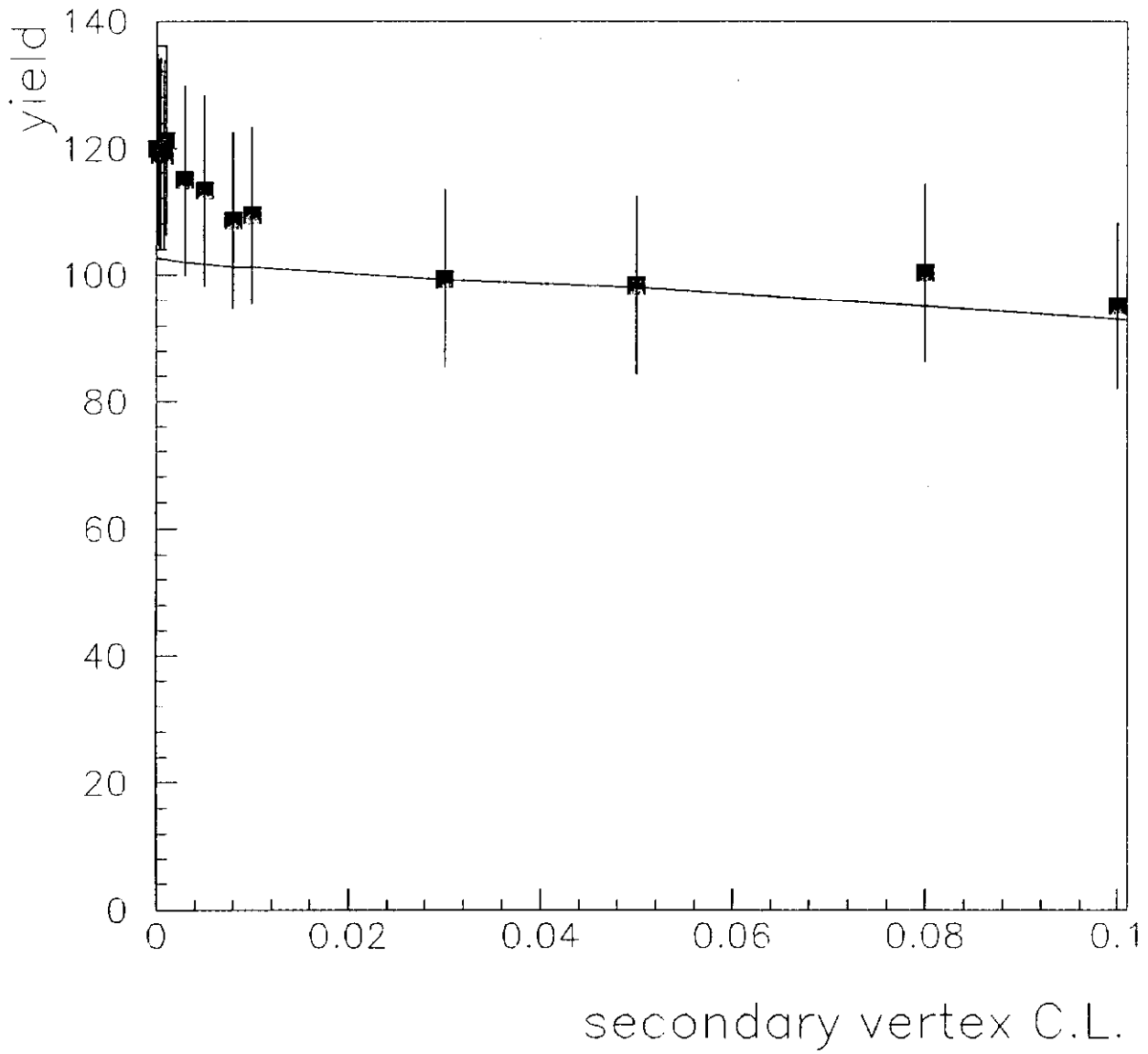


Fig. 4: Number of events in the D^* peak (random background subtracted) as a function of the secondary vertex confidence level; the full line is the Monte Carlo prediction; the cut chosen is 0.05.

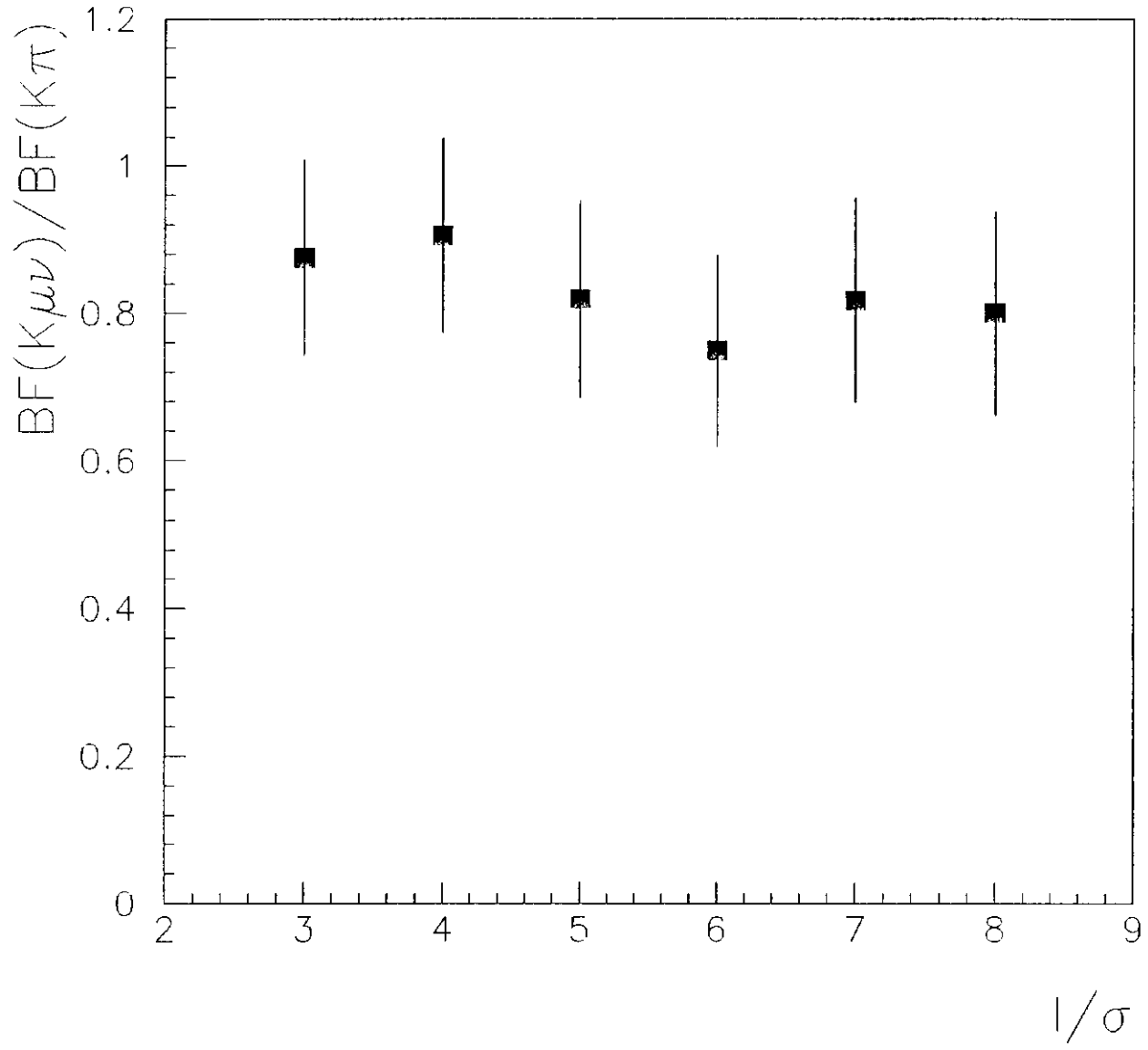


Fig. 5: Branching ratio value as a function of the ℓ/σ_ℓ cut.

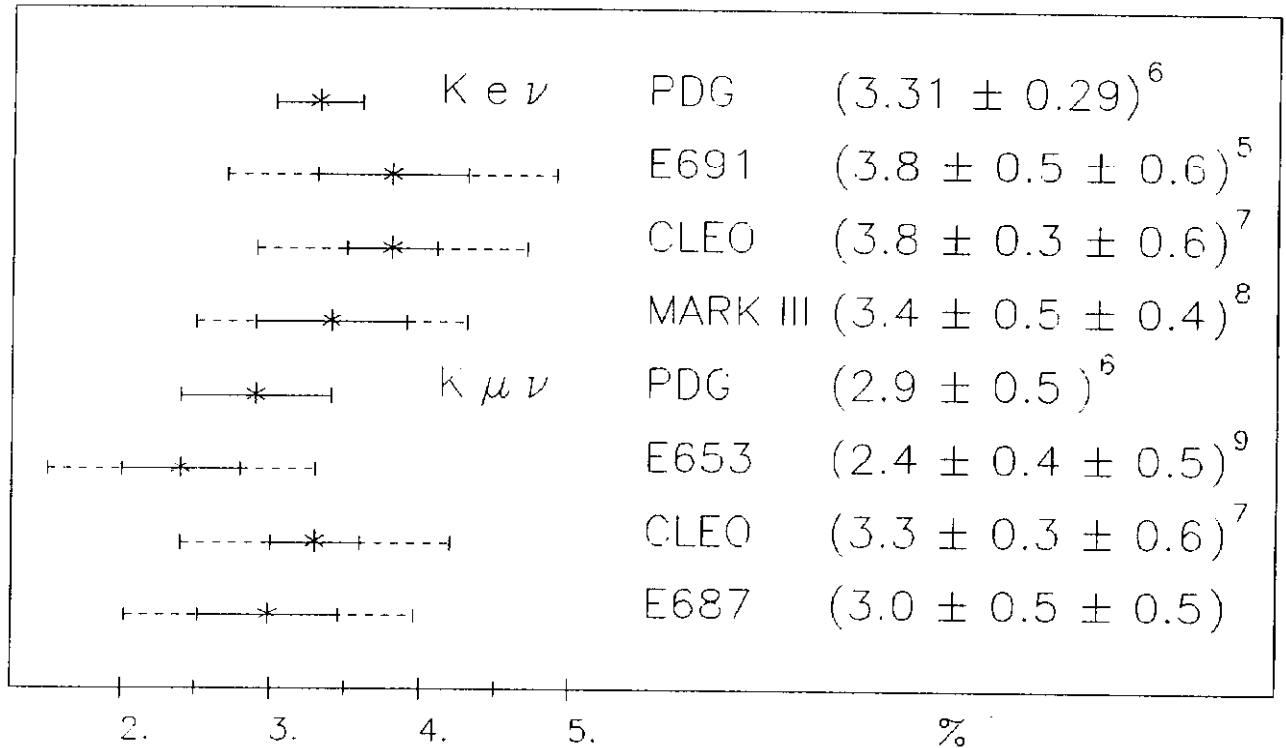


Fig. 6: Comparison of $BF(D^0 \rightarrow K^- l^+ \nu)$ measurements (values are in %): the statistical (full line) and systematic errors are summed linearly (dashed line). The E691^[5] and CLEO^[7] values have been obtained using the Mark III value for the $BF(D^0 \rightarrow K^- \pi^+)$; E653^[9] calculates this value from the branching ratio $\Gamma(D^0 \rightarrow K \mu \nu)/\Gamma(D^0 \rightarrow X \mu \nu)$.

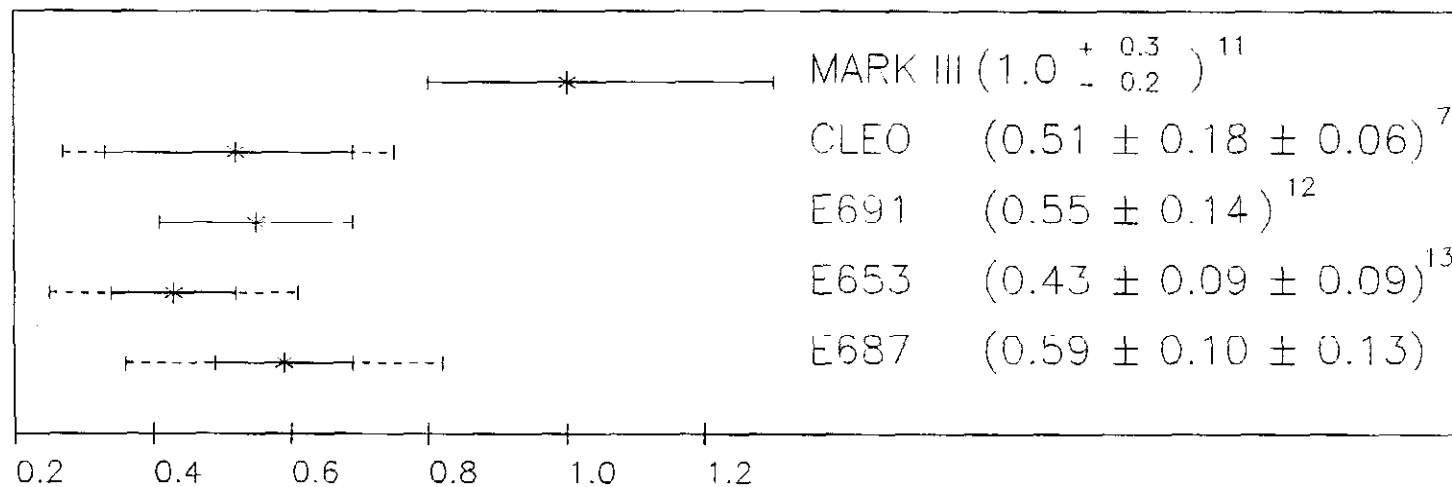


Fig. 7: Comparison of $\Gamma(D^0 \rightarrow K^{*-}l^+\nu)/\Gamma(D^0 \rightarrow K^-l^+\nu)$ measurements: the statistical (full line) and systematic errors are summed linearly (dashed line). Mark III value refers to the $Kl4/Kl3$ ratio: they do not have sufficient sensitivity to quote a branching fraction ratio for the $D^0 \rightarrow K^{*-}l^+\nu$ ^[14].